THE BELL SYSTEM TECHNICAL JOURNAL
Vol. 54, No. 1, January 1975
Printed in U.S.A.

Quasi-Ray Analysis of Crosstalk Between Multimode Optical Fibers

By A. H. CHERIN and E. J. MURPHY

(Manuscript received April 3, 1974)

A model based on frustrated total reflection of waves in a multilayered medium has been developed to analyze the crosstalk between multimode optical fibers. Kappa (κ), the parameter indicating the power distribution among the modes of the fiber, and fiber cladding thickness play very important roles in determining the crosstalk isolation between fibers. Significant but less dominant effects on crosstalk are due to variations in fiber numerical aperture, length, and transmitting wavelength.

I. INTRODUCTION

Crosstalk between communications circuits has long been a problem concerning engineers and designers in the telecommunications industry. In a digital communications system using optical fibers as a transmission medium, at least a 30-dB signal-to-crosstalk ratio will be needed. In those applications where a lossy jacket around the fiber is undesirable, proper design of optical fiber cables and circuits requires an understanding of the parameters that control crosstalk between the fibers.

A number of models can be found in the literature to describe crosstalk between optical fibers.[1–8] Maxwell's equations are the usual starting point for these models, and a field theory approach describing the coupling coefficients between individual modes results. Each of these models provides insight into a possible mechanism for describing crosstalk between optical fibers, and each is operationally useful for calculating crosstalk between single-mode fibers or guides with a small number of propagating modes. A very interesting model describing crosstalk resulting from scattering from a rough core-cladding interface is also described in the literature.[9]

In this paper, a meridional quasi-ray tracing procedure is used to describe crosstalk between highly multimoded optical fibers. This approach is an extension of work developed by H. P. Yuen[10] and N. S. Kapany.[11–14] The mechanism for crosstalk coupling of energy between fibers is that of frustrated total internal reflection of waves in a multi-

layered medium. Integral expressions for crosstalk and transmitted power are developed in terms of the geometry of the system, the absorption loss of the fiber cores, the transmission and reflection coefficients at the core-cladding interface, and the energy distribution at the launching end of the fiber. It is assumed in this work that the propagating modes within a fiber are uncoupled. The error resulting from this assumption should be small when the excitation is chosen to coincide with the equilibrium energy distribution and the coupling between the fibers is weak. A computer evaluation has been made of the integral expressions for crosstalk and transmitted power. Results of a study showing the functional relationship between far-end equal-level crosstalk (FEXT) and cladding thickness, mode energy distribution, length, numerical aperture, and wavelength are included in this paper, along with a discussion of future work in this area.

II. DERIVATION OF GENERAL TRANSMISSION AND CROSSTALK FORMULAS

For the system of fibers shown in Fig. 1, we present a general derivation of the transmission of energy within a fiber and the crosstalk behavior between fibers. We assume that each fiber in an assembly is excited by a source that focuses its power on the center of the entrance end of a fiber, exciting meridional rays as shown in Fig. 2. The ray incident at an angle θ_o to the axis of the fiber is refracted into the fiber at an angle θ which can be simply related to θ_o by the law of refraction. Consider a distribution of input radiant intensity or input power per unit solid angle $F_o(\theta, \phi)$ for some polar angle defined on the entrance surface. A certain fraction of the power, $T_o(\theta, \phi)$, will be transmitted into the fiber because of refraction at the entrance surface. Within the incremental solid angle, $\sin \theta d\theta d\phi$, the power coupled into the fiber, $dP(\theta, \phi)$, can be written as

$$dP(\theta, \phi) = F(\theta, \phi) \sin \theta d\theta d\phi = F_o(\theta, \phi) T_o(\theta, \phi) \sin \theta d\theta d\phi \quad (1)$$

or

$$\left(\frac{dP(\theta, \phi)}{d\Omega} \right)_{\text{entrance}} = F(\theta, \phi). \quad (1a)$$

We assume here that an absorption coefficient α per unit length is defined for the fibers. The coefficient α takes into account both bulk absorption loss and scattering loss.

The power flux just prior to hitting the core-cladding interface of the fiber for the first time is given by

$$\left(\frac{dP}{d\Omega} \right)_{P_1} = \epsilon^{-\alpha (d/2) \csc \theta} F(\theta, \phi), \quad (2)$$

where d is the fiber core diameter.

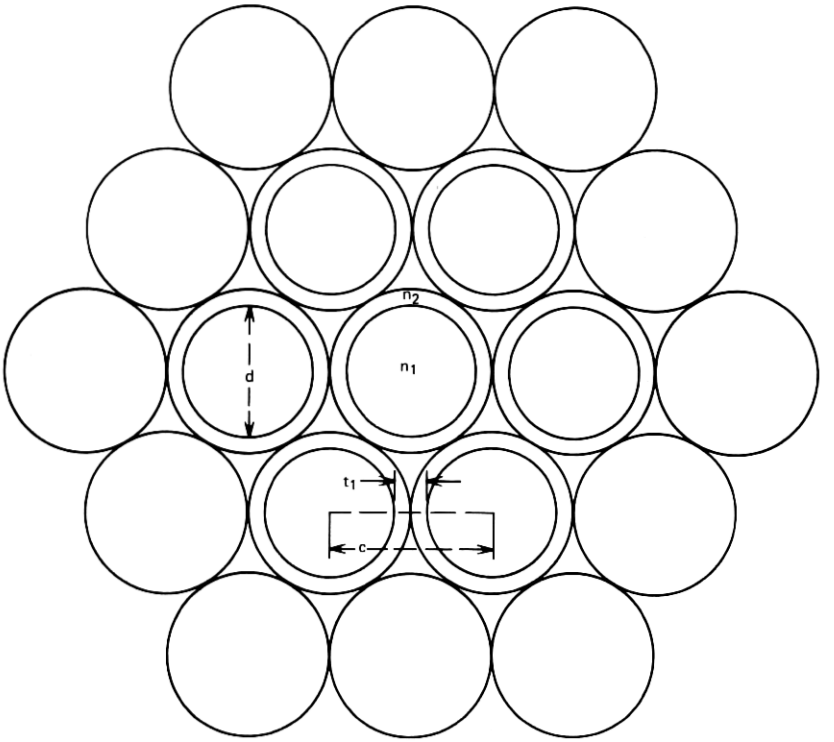

Fig. 1—System of optical fibers.

The power reflected from the first reflection at the core-cladding interface can then be written as

$$\left(\frac{dP}{d\Omega}\right)_{R_1} = \epsilon^{-\alpha(d/2)\csc\theta} R(\theta, \phi) F(\theta, \phi). \tag{3}$$

The power transmitted into a neighboring fiber from the first reflection at the interface is given by:

$$\left(\frac{dP}{d\Omega}\right)_{T_1} = \epsilon^{-\alpha(d/2)\csc\theta} T(\theta, \phi) F(\theta, \phi). \tag{4}$$

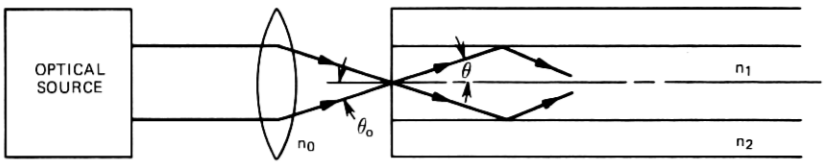

Fig. 2—Meridional ray fiber excitation.

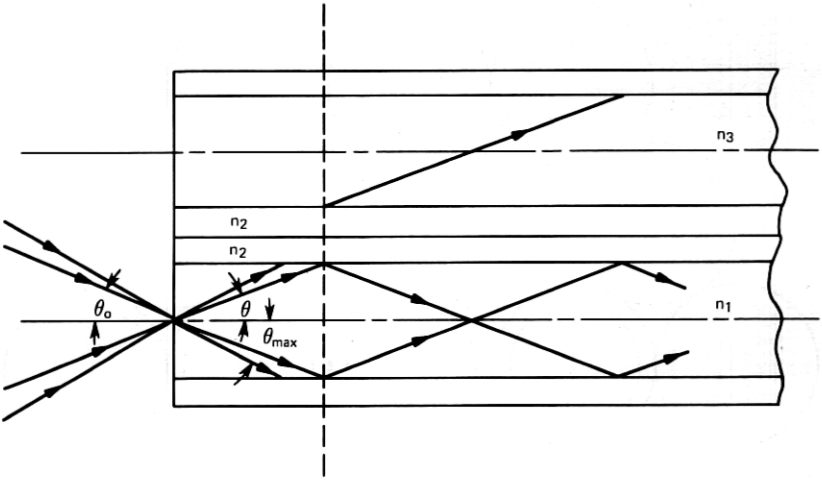

Fig. 3—Ray tracing of transmitted and crosstalk rays in adjacent optical fibers.

The next section shows how $R(\theta, \phi)$, the reflection coefficient, and $T(\theta, \phi)$, the transmission coefficient, are calculated. $T(\theta, \phi)$ in this study is, in effect, the mechanism for obtaining crosstalk between fibers. Crosstalk is shown to be caused by frustrated total reflection of plane waves at the interface of a multilayered medium. The reflected rays continue their propagation down the fiber until they hit the wall again. A fraction of energy is then tunneled as crosstalk to the neighboring fibers, and another fraction is reflected. This process is repeated until the rays reach the exit end of the fiber, as illustrated in Fig. 3. Let us make the following definitions:

$$\left(\frac{dP}{d\Omega}\right)_{P_n} \equiv \text{incident power density at the } n\text{th hit}$$

$$\left(\frac{dP}{d\Omega}\right)_{T_n} \equiv \text{transmitted power density at the } n\text{th hit}$$

$$\left(\frac{dP}{d\Omega}\right)_{R_n} \equiv \text{reflected power density at the } n\text{th hit.}$$

The following power expressions for the nth hit clearly hold.

$$\left(\frac{dP}{d\Omega}\right)_{T_n} = \left(\frac{dP}{d\Omega}\right)_{P_n} T(\theta, \phi) \tag{5}$$

$$\left(\frac{dP}{d\Omega}\right)_{R_n} = \left(\frac{dP}{d\Omega}\right)_{P_n} R(\theta, \phi) \tag{6}$$

$$\left(\frac{dP}{d\Omega}\right)_{P_{n+1}} = \left(\frac{dP}{d\Omega}\right)_{R_n} \epsilon^{-\alpha d \csc\theta}. \tag{7}$$

For a ray of angle θ relative to the fiber axis, the total number of hits M is the largest integer smaller than $(L/d)(\tan\theta) + \frac{1}{2}$.

$$M = \left[\frac{L}{d}\tan\theta + \tfrac{1}{2}\right] \tag{8}$$

and the total path length is $L \sec\theta$. The output power distribution at the exit end is therefore

$$\left(\frac{dP}{d\Omega}\right)_{\text{output}} = \epsilon^{-\alpha L\sec\theta} R^M(\theta, \phi)F(\theta, \phi), \tag{9}$$

so that the total output power of the fiber is

$$P_{\text{output}} = \int_o^{2\pi}\int_o^{\theta_{\max}} \sin\theta F(\theta, \phi)R^M(\theta, \phi)\epsilon^{-\alpha L\sec\theta}T_o(\theta, \phi)d\theta d\phi. \tag{10}$$

If the exit end of the fiber is not matched to the surrounding medium, there is a transmission factor, $T_o(\theta, \phi) \neq 1$. From eqs. (2), (5), (6), and (7), we obtain

$$\left(\frac{dP}{d\Omega}\right)_{T_n} = \epsilon^{-\alpha d(n-\frac{1}{2})\csc\theta}[R(\theta, \phi)]^{n-1}T(\theta, \phi)F(\theta, \phi). \tag{11}$$

Let each crosstalk ray at the nth hit suffer a further attenuation $A'(\theta, \phi, L, n)$ before it reaches the exit end. The total crosstalk output power is then given by

$$P_{xt} = \int_o^{2\pi}\int_o^{\theta_{\max}} \sin\theta F(\theta, \phi)T(\theta, \phi) \times \sum_{n=1}^{M}[R(\theta, \phi)]^{n-1}A'(\theta, \phi, L, n)\epsilon^{-\alpha d(n-\frac{1}{2})\csc\theta}d\theta d\phi. \tag{12}$$

Note that M is a function of θ. Equations (10) and (12) provide the general formula for signal and crosstalk output power at the end of the fiber as a function of the system parameters. For a specific model of the crosstalk transfer, it is necessary to provide explicit expressions for $F(\theta, \phi)$, $R(\theta, \phi)$, $T(\theta, \phi)$, and $A'(\theta, \phi, L, n)$. A very simple model is discussed later in this paper.

That quantity of particular interest in system design is the signal-to-crosstalk power ratio defined by

$$\left(\frac{S}{N}\right)_{\text{XT}} = \frac{P_{\text{output}}}{P_{\text{XT}}}. \tag{13}$$

Far-end equal-level crosstalk in decibels is then defined as

$$\text{FEXT} = 10\log_{10}\frac{P_{\text{output}}}{P_{\text{XT}}}. \tag{14}$$

III. FRUSTRATED TOTAL INTERNAL REFLECTION IN A MULTILAYERED MEDIUM—A CROSSTALK MECHANISM

In this section, a discussion is given of frustrated total reflection of plane waves in a multilayer medium. This mechanism is the one responsible for crosstalk in our model and serves as the basis for our crosstalk power transmission calculation.

Consider the usual representation of total internal reflection shown in Fig. 4. The ray is completely reflected when ψ exceeds the critical angle, $\psi_c = \sin^{-1}(n_2/n_1)$. The field amplitude decays exponentially in the optically rarer medium. This picture is quite different when we look at the energy flow of the waves more closely.[15–17] The Poynting vector in the rarer medium is by no means zero; only its time average vanishes. This energy flow is depicted in Fig. 5, which also shows that a displacement Δ exists, because of the Goos-Hänchen shift,[15,16] between the incident and reflected beam. For plane waves, this shift is readily calculated.[15] It increases with decreasing angle of incidence ψ, as expected. The Poynting vector also makes a deeper penetration when ψ is smaller.

With this picture we can see that, if a third medium of refractive index, n_1, is brought into close proximity to the first surface from below, as shown in Fig. 6, some energy will be trapped by it as the incident rays make their penetration. This trapped energy will then propagate

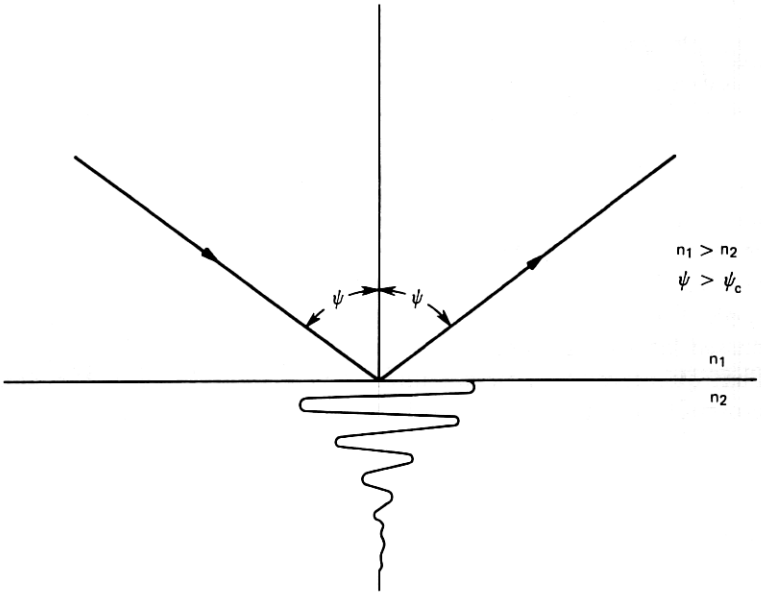

Fig. 4—Total internal reflection from plane dielectric boundary.

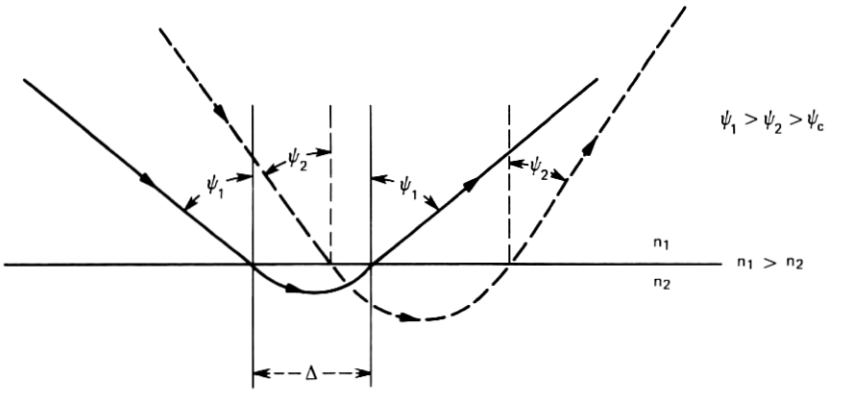

Fig. 5—Displacement of ray—the Goos-Hänchen shift.

into the third medium. This phenomenon of energy transmission through a lower refractive index slab for incidence greater than the critical angle is called frustrated total internal reflection. It is a wave phenomenon outside the domain of pure geometrical optics and is exactly analogous to the tunneling of quantum mechanical particles through a potential barrier, which is classically forbidden.

Consider now three homogeneous media that might represent the core, claddings, and core of adjacent fibers and model them by two half spaces of refractive index, n_1, separated by a third medium, n_2, of thickness, t. We have three homogeneous media for which the transmission coefficient can be obtained by matching boundary conditions directly. The result, for plane wave incidence, is well known in the

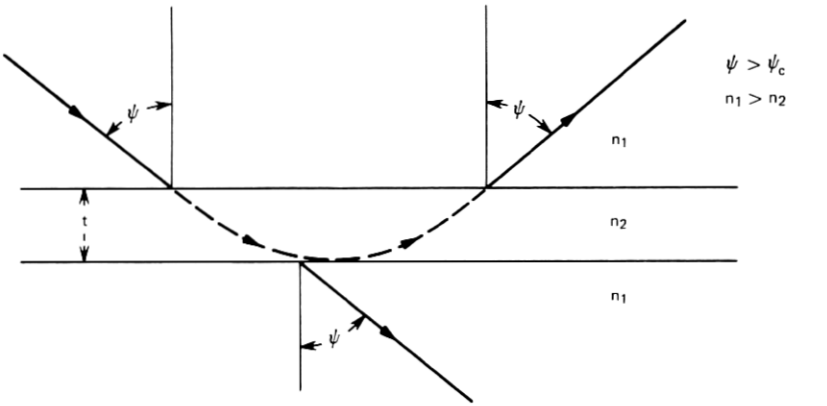

Fig. 6—Frustrated total internal reflection in a multilayered dielectric medium.

literature[15] and has been derived in the appendix for the N media case and specialized to the three-media case discussed here. We assume that, in the vicinity of the core-cladding interface, the signal can be represented as a plane wave and quote the result for the lossless case for the geometry and notation shown in Fig. 7.

Let

$$\gamma = \left[\left(\frac{n_1}{n_2}\right)^2 \sin^2 \theta_1 - 1\right]^{\frac{1}{2}}. \tag{15}$$

The transmission coefficient, $T(\theta, t)$, which can be defined as the ratio of the transmitted power flux to the incident power flux, is given by

$$T(\theta, \phi) = \left[A_1 \frac{1}{\cosh^2 \beta + [(n_2\gamma^2 - n_1 \cos^2 \theta_1)/2n_1n_2 \cos \theta_1\gamma]^2 \sinh^2 \beta}\right] + A_2\left[\frac{1}{\cosh^2 \beta + [(n_2^2 \cos^2 \theta_1 - \gamma 2n_1)/2 \cos \theta_1 n_1 n_2 \gamma]^2 \sin^2 h\beta}\right], \tag{16}$$

where

A_1 = the fraction of incident power polarized perpendicular to the plane of incidence.

A_2 = the fraction of incident power polarized parallel to the plane of incidence.

$$\beta = \frac{2\pi}{\lambda} n_2 t\gamma. \tag{17}$$

Formula (16) is written in terms of θ_o, the incident angle at the input of the fiber, and is used in the calculation of crosstalk power later in this paper.

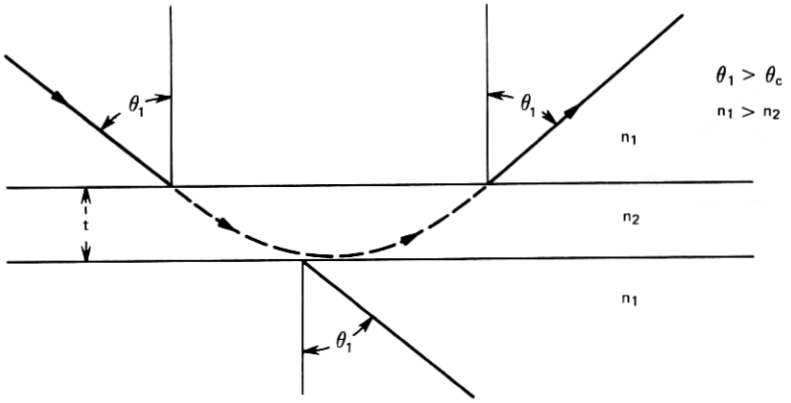

Fig. 7—Geometry for calculation of transmission and reflection coefficients in a single-layered three-medium dielectric.

IV. CROSSTALK FORMULA ADAPTED TO CIRCULAR GEOMETRY

We assume now that the only crosstalk that is modeled here is that which is due to frustrated total reflection. The geometry of the rays near the fiber wall at a hit is illustrated in Fig. 8, which is a cross-sectional view of a fiber and one of its neighbors. Here, ϕ is the polar angle which also serves to define the length t. Using simple geometry we see that

$$t = c \cos \phi - d/2 - [(d/2)^2 - c^2 \sin^2 \phi]^{\frac{1}{2}} \tag{18}$$

and that the angle ϕ_m for which the line ON is tangent to the circle O' is

$$\phi_m = \sin^{-1} d/2c. \tag{19}$$

Let E denote the center point of the entrance end of the fiber. Then a meridional ray ES hitting the wall of the fiber lies in the plane of inci-

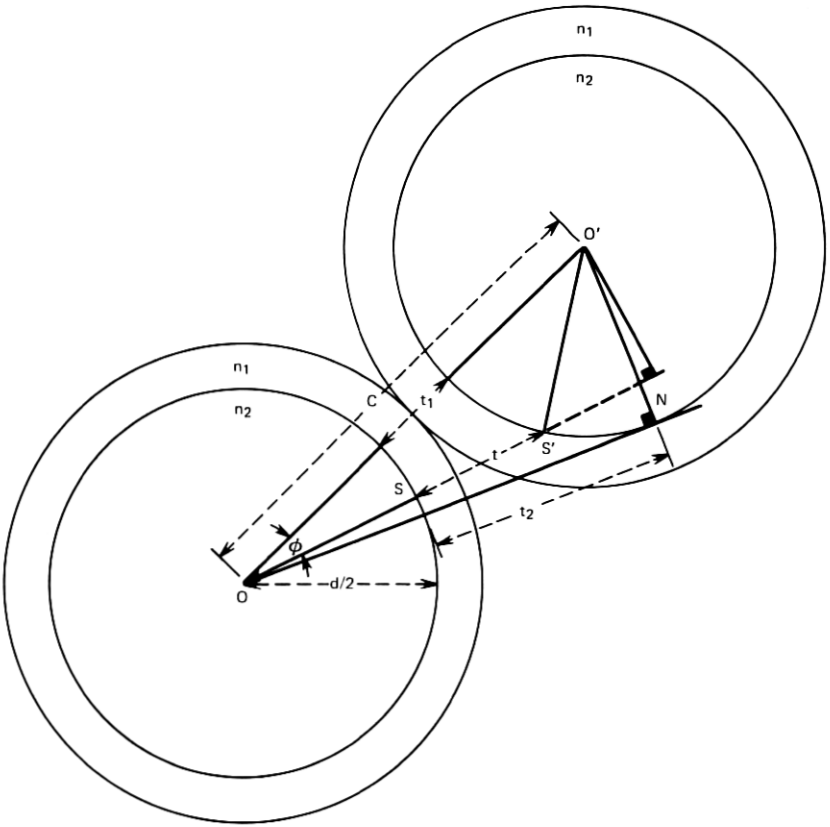

Fig. 8—Geometry of two adjacent round optical fibers.

dence EOS, which cuts the fiber O' at a line passing through S' parallel to the axis of the fiber. The transmission coefficient is calculated in the form of plane wave tunneling through a slab of thickness t, as in Fig. 7. When the medium between is homogeneous and lossless, eq. (16) can be used.

The transmitted ray will propagate as a skew ray and emerge from a point a number of wavelengths from S' depending on θ, as is clear from Figs. 5 and 7. Since the displacement Δ is small compared to the path length between bounces and very small compared to the length of fiber we are interested in, we can essentially regard the ray to emerge from S' for the purpose of calculating the path length of the transmitted ray.

Skew ray analysis shows[12] that the length of the skew ray crosstalk path lengths are also given by $L \sec \theta$. We can now calculate the expressions for P_{XT} and P_{output}. From the above discussion, substitution into the crosstalk integral, eq. (12), yields

$$A'(n)\epsilon^{-ad(n-\frac{1}{2})\csc\theta} = \epsilon^{-\alpha L \sec\theta} \tag{20}$$

and

$$\sum_{n=1}^{M} [R(\theta, \phi)]^{n-1} A'(n)\epsilon^{-ad(n-\frac{1}{2})\csc\theta} = \epsilon^{-\alpha L\sec\theta} \sum_{n=1}^{M} R(\theta, \phi)^{n-1}$$
$$= \epsilon^{-\alpha L\sec\theta}\left[\frac{1 - R(\theta, \phi)^M}{1 - R(\theta, \phi)}\right]. \tag{21}$$

The crosstalk integral simplifies to

$$P_{XT} = \int_o^{\theta_{max}} d\theta \int_o^{2\pi} d\phi \sin\theta F(\theta, \phi)\epsilon^{-\alpha L\sec\theta} T(\theta, \phi) \times \left[\frac{1 - R(\theta, \phi)^M}{1 - R(\theta, \phi)}\right]. \tag{22}$$

Making a change of variable to t with

$$\frac{d\phi}{dt} = \frac{c^2 - (d/2)^2 - (t + d/2)^2}{(t + d/2)\{(c^2 - t^2)[(t + d)^2 - c^2]\}^{\frac{1}{2}}}, \tag{23}$$

we can then write

$$P_{XT} = N\int_o^{\theta_{max}} d\theta \int_{t_1}^{t_2} dt \left(\frac{d\phi}{dt}\right) \sin\theta F(\theta, t)\epsilon^{-\alpha L\sec\theta} T(\theta, t) \times \left[\frac{1 - R(\theta, t)^M}{1 - R(\theta, t)}\right], \tag{24}$$

where $N = 2$ times the number of fibers adjacent to the excited fiber.

V. SIMPLIFIED CROSSTALK FORMULAS USED FOR INITIAL COMPUTER STUDY

A specific model requires a knowledge of $F(\theta, \phi)$, $R(\theta, \phi)$, and $T(\theta, \phi)$ in eqs. (24) and (10) to calculate the crosstalk between fibers. As a first-order approximation, the following assumptions were made:

(*i*) The interfiber medium is lossless and homogeneous so that eq. (16) is valid as well as:

(*ii*)
$$T(\theta, \phi) + R(\theta, \phi) = 1. \tag{25}$$

(*iii*) The input angular power distribution of the fiber is a gaussian function of the form

$$F(\theta, \phi) = \epsilon^{-(\theta/\kappa\theta_c)^2}, \tag{26}$$

where κ is a parameter that is a measure of the width of the beam and also an indication of how the power is distributed between the modes of the fiber. θ_c is the critical angle of the fiber.

(*iv*) The air spaces between the fibers are replaced by cladding material for the purposes of calculating the transmission coefficient, $T(\theta, \phi)$. A partial check of this assumption showed that the primary contribution to crosstalk occurred for small values of ϕ. Replacing the air spaces by cladding material caused a maximum error in crosstalk of 4.5 dB.

Under the assumptions mentioned above, the crosstalk integral, (24), becomes

$$P_{XT} = N \int_o^{\theta_{max}} d\theta \int_{t_1}^{t_2} dt \left(\frac{d\phi}{dt} \right) \times \sin \theta \epsilon^{-(\theta/\kappa\theta_c)^2} \epsilon^{-\alpha L \sec\theta} \{1 - [1 - T(\theta, t)]^M\}. \tag{27}$$

The total output power of the transmitting fiber becomes

$$P_{output} = \int_o^{2\pi} d\phi \int_o^{\theta_{max}} \sin \theta \epsilon^{-(\theta/\kappa\theta_c)^2} \epsilon^{-\alpha L \sec\theta} [1 - T(\theta, \phi)]^M d\theta. \tag{28}$$

VI. COMPUTER STUDY—SUMMARY OF RESULTS

A computer program was written and the integrals (27) and (28) were evaluated for typical fiber parameters. A number of studies were made to determine how FEXT [eq. (14)] varies as a function of cladding thickness, numerical aperture, length, κ (kappa), and wavelength. Table I is a guide that defines the parameters and relates the variables

Table I

Far-End Crosstalk as a Function of	Figure Number	Parameters Held Constant	Range of Independent Variable
$\frac{d}{c} - \frac{\text{Core Diam}}{\text{Cladding Diam}}$	9	NA = 0.10, d = 25.4 μm, L = 1 km, λ = 0.6328 μm α = 20 dB/km, κ = 0.25, 0.35, 0.4, 0.5, 10.0	$\frac{d}{c}$ – 0.3 to 0.7
$\frac{d}{c}$	10	NA = 0.15, d = 25.4 μm, L = 1 km, λ = 0.6328 μm α = 20 dB/km, κ = 0.25, 0.35, 0.4, 0.5, 10.0	$\frac{d}{c}$ – 0.3 to 0.7
$\frac{d}{c}$	11	NA = 0.20, d = 25.4 μm, L = 1 km, λ = 0.6328 μm α = 20 dB/km, κ = 0.25, 0.35, 0.4, 0.5, 10.0	$\frac{d}{c}$ – 0.3 to 0.7
$\frac{d}{c}$	12	NA = 0.10, d = 50.8 μm, L = 1 km, λ = 0.6328 μm α = 20 dB/km, κ = 0.25, 0.35, 0.4, 0.5, 10.0	$\frac{d}{c}$ – 0.5 to 0.9
$\frac{d}{c}$	13	NA = 0.15, d = 50.8 μm, L = 1 km, λ = 0.6328 μm α = 20 dB/km, κ = 0.25, 0.35, 0.4, 0.5, 10.0	$\frac{d}{c}$ – 0.5 to 0.9
$\frac{d}{c}$	14	NA = 0.20, d = 50.8 μm, L = 1 km, λ = 0.6328 μm α = 20 dB/km, κ = 0.25, 0.35, 0.4, 0.5, 10.0	$\frac{d}{c}$ – 0.5 to 0.9
$\frac{d}{c}$	15	NA = 0.10, d = 76.2 μm, L = 1 km, λ = 0.6328 μm α = 20 dB/km, κ = 0.25, 0.35, 0.4, 0.5, 10.0	$\frac{d}{c}$ – 0.5 to 0.9
$\frac{d}{c}$	16	NA = 0.15, d = 76.2 μm, L = 1 km, λ = 0.6328 μm α = 20 dB/km, κ = 0.25, 0.35, 0.4, 0.5, 10.0	$\frac{d}{c}$ – 0.5 to 0.9
$\frac{d}{c}$	17	NA = 0.20, d = 76.2 μm, L = 1 km, λ = 0.6328 μm α = 20 dB/km, κ = 0.25, 0.35, 0.4, 0.5, 10.0	$\frac{d}{c}$ – 0.5 to 0.9
Numerical aperture	18	d = 50.8 μm, c = 85 μm, α = 20 dB/km, L = 1 km, λ = 0.6328 μm, κ = 0.25, 0.35, 0.40, 0.50, 10.0	NA = 0.05 to 0.30
Fiber length	19	d = 50.8 μm, c = 85 μm, α = 20 dB/km, NA = 0.15 λ = 0.6328 μm, κ = 0.25, 0.35, 0.4, 0.5, 10.0	L = 100 m to 5 km
κ (Kappa)	20	L = 1 km, d = 50.8 μm, c = 85 μm, α = 20 dB/km NA = 0.15, λ = 0.6328 μm	κ = 0.1 to 1.0
Wavelength	21	L = 1 km, d = 50.8 μm, c = 85 μm, α = 20 dB/km NA = 0.15, κ = 0.25, 0.35, 0.4, 0.5, 10.0	λ = 0.6328 to 1.06 μm

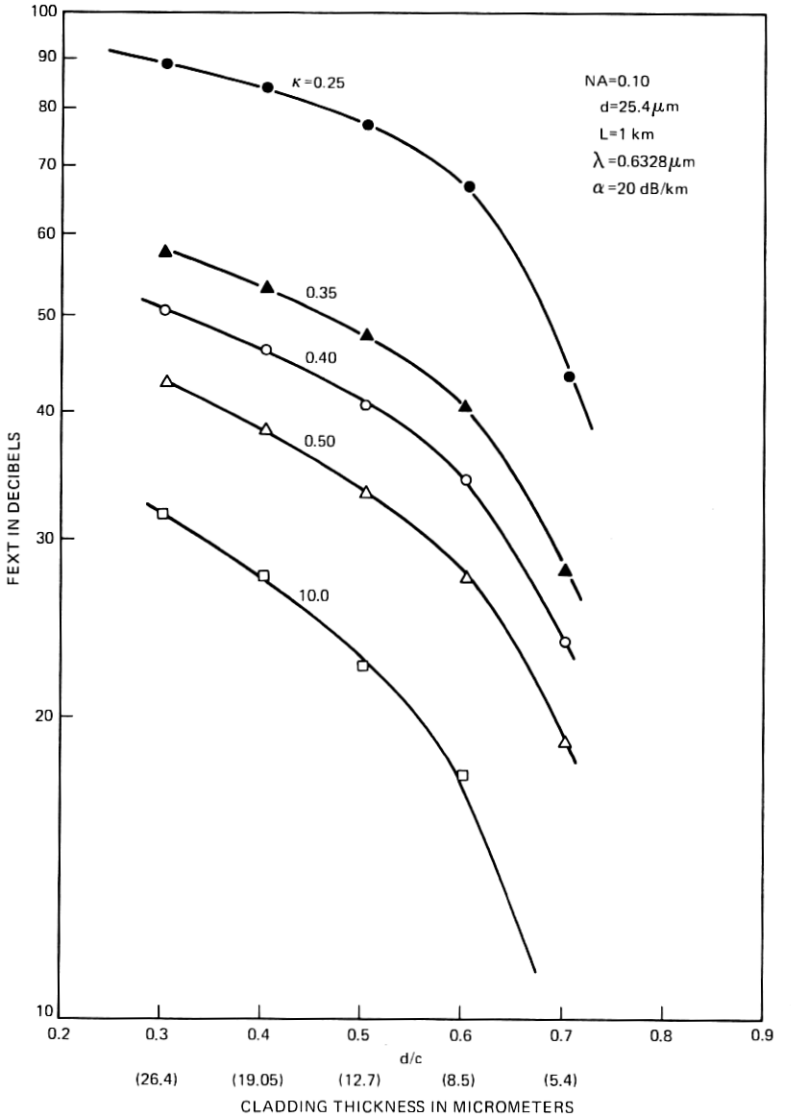

Fig. 9—FEXT vs. d/C (cladding thickness), d = 25.4 μm, NA = 0.10, L = 1 km, λ = 0.6328 μm, α = 20 dB/km.

in the study to the figure numbers appearing in this paper. Figures 9 to 11 show, for numerical apertures of 0.10, 0.15, and 0.20, respectively, the relationships between FEXT and cladding thickness for a 1-mil fiber core diameter. For the same numerical apertures, Figs. 12 to 14 and 15 to 17 show this relationship for 2- and 3-mil core diameters.

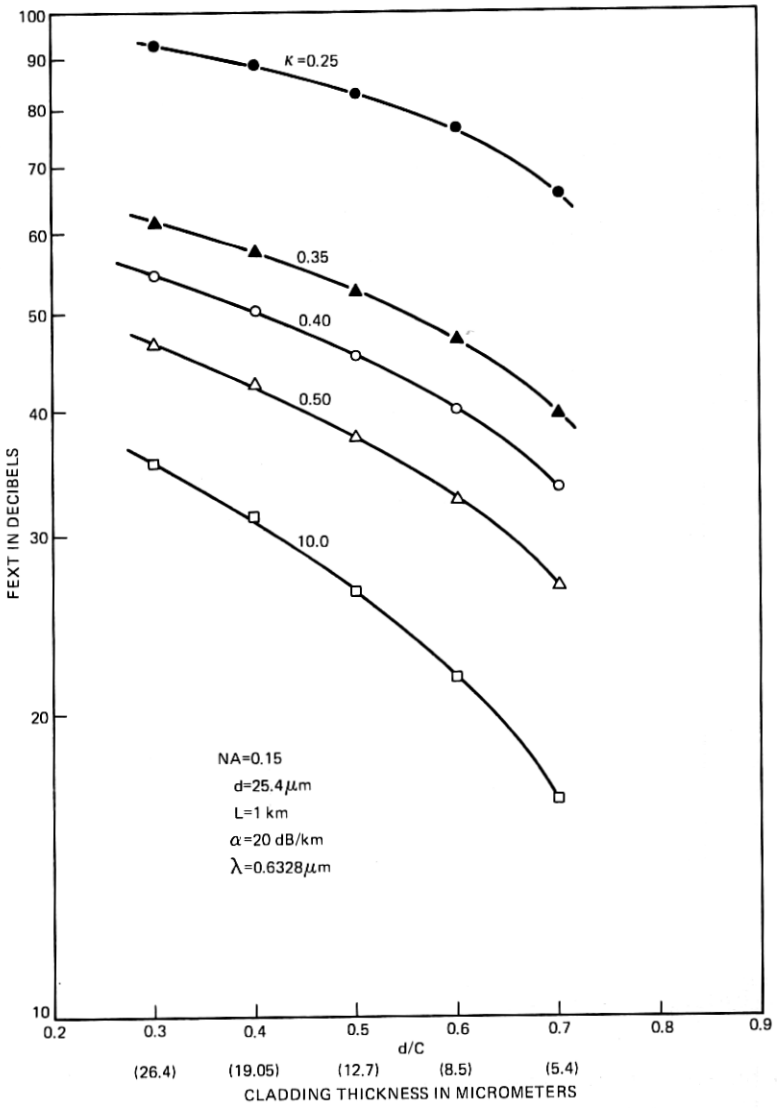

Fig. 10—FEXT vs. d/C (cladding thickness), $d = 25.4$ μm, NA = 0.15, $L = 1$ km, $\lambda = 0.6328$ μm, $\alpha = 20$ dB/km.

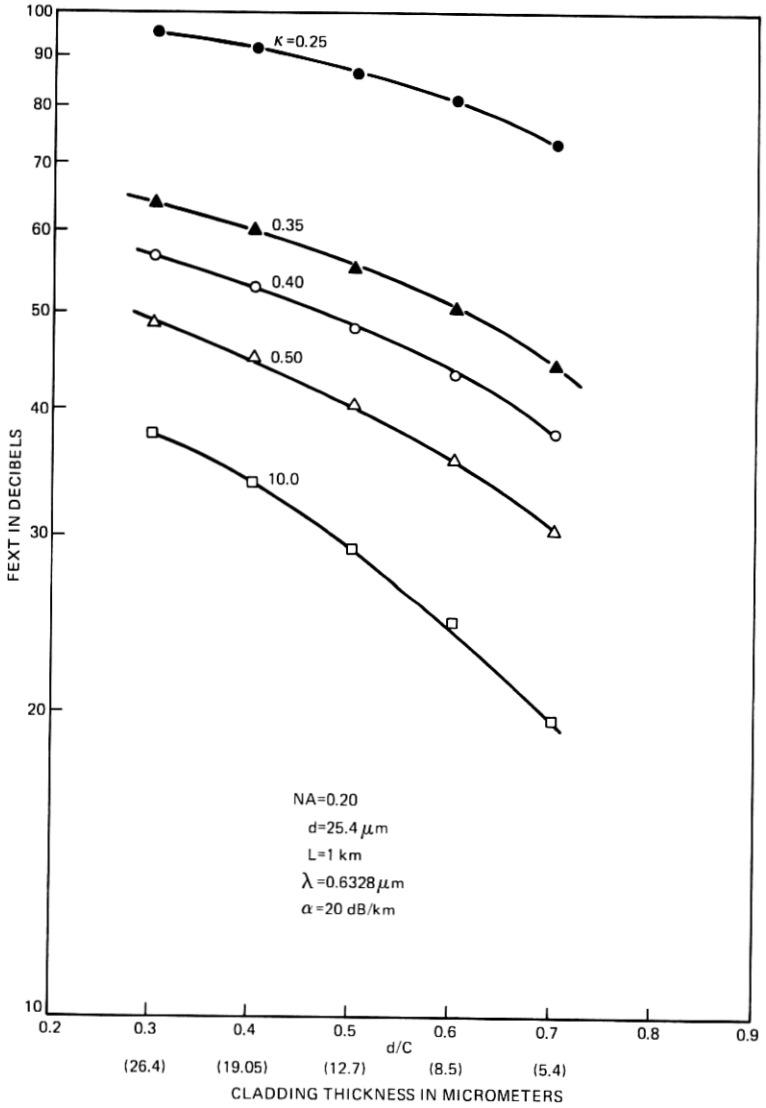

Fig. 11—FEXT vs. d/C (cladding thickness), $d = 25.4$ μm, NA = 0.20, $L = 1$ km, $\lambda = 0.6328$ μm, $\alpha = 20$ dB/km.

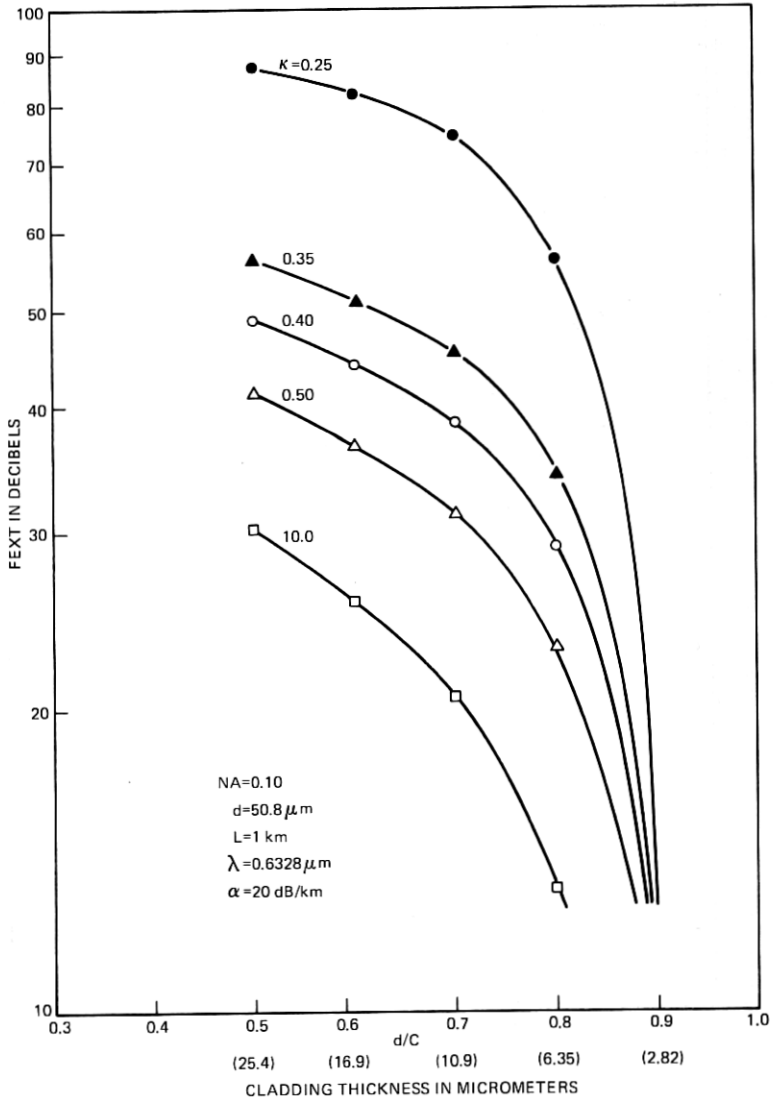

Fig. 12—FEXT vs. d/C (cladding thickness), $d = 50.8$ μm, NA = 0.10, $L = 1$ km, $\lambda = 0.6328$ μm, $\alpha = 20$ dB/km.

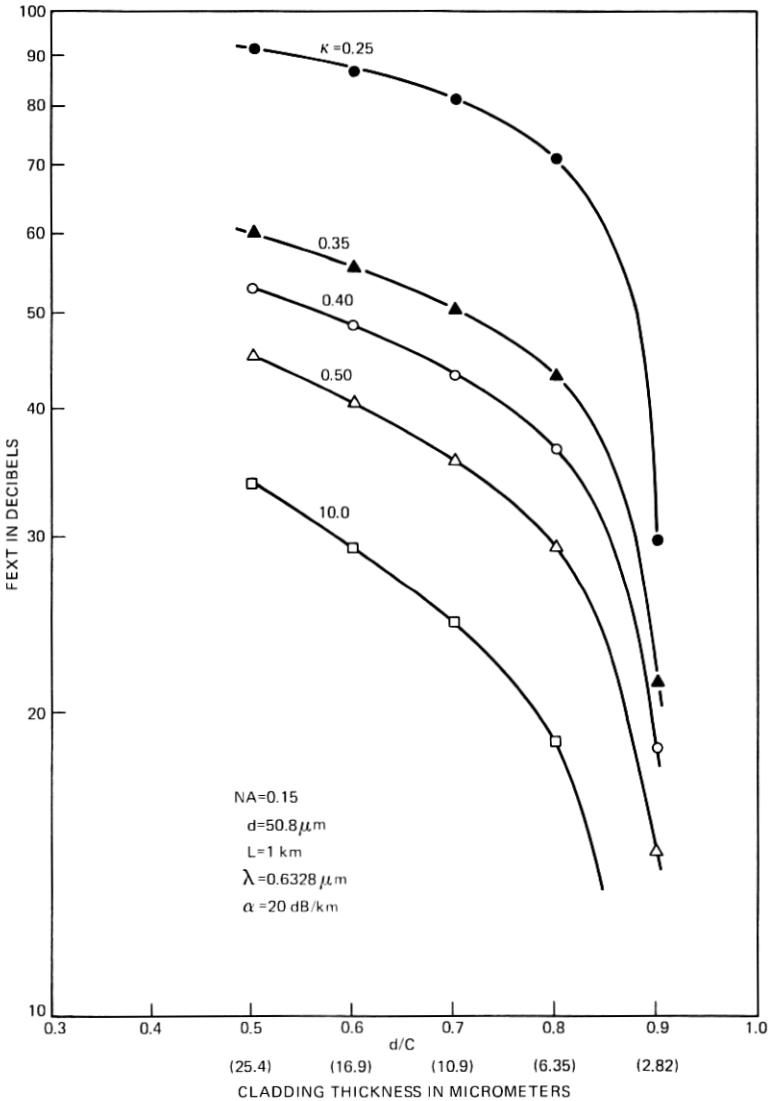

FIG. 13—FEXT vs. d/C (cladding thickness), $d = 50.8$ μm, NA = 0.15, $L = 1$ km, $\lambda = 0.6328$ μm, $\alpha = 20$ dB/km.

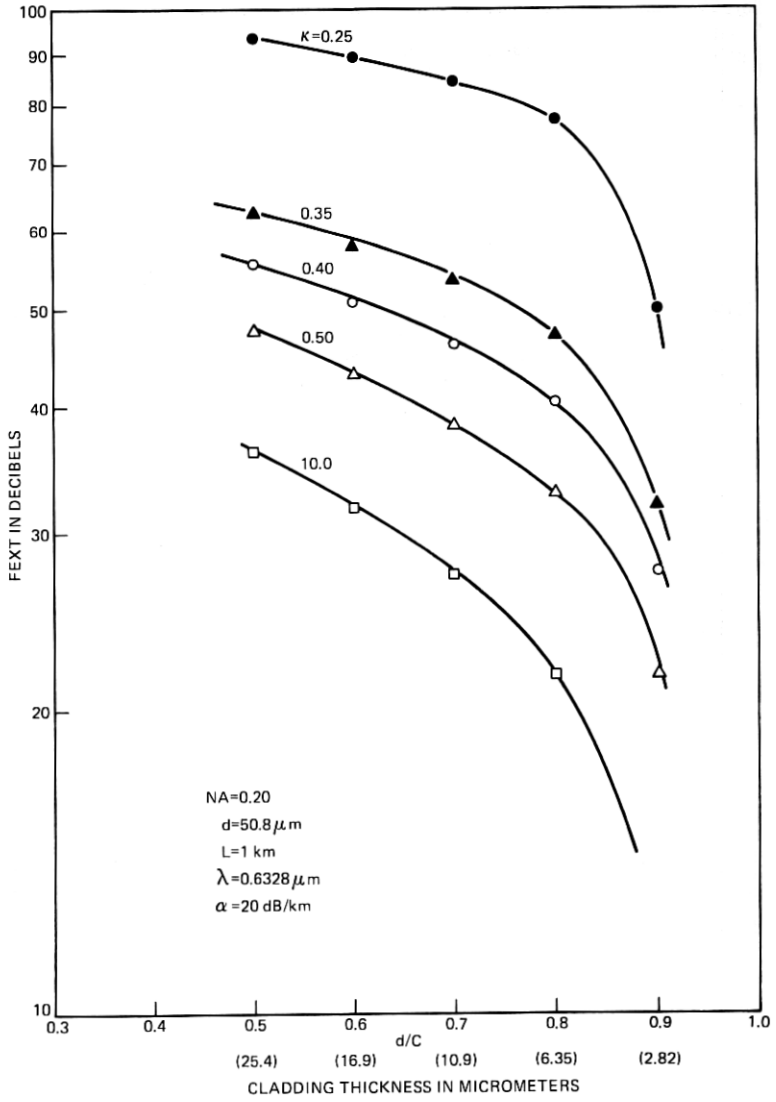

Fig. 14—FEXT vs. d/C (cladding thickness), $d = 50.8$ μm, NA = 0.20, $L = 1$ km, $\lambda = 0.6328$ μm, $\alpha = 20$ dB/km.

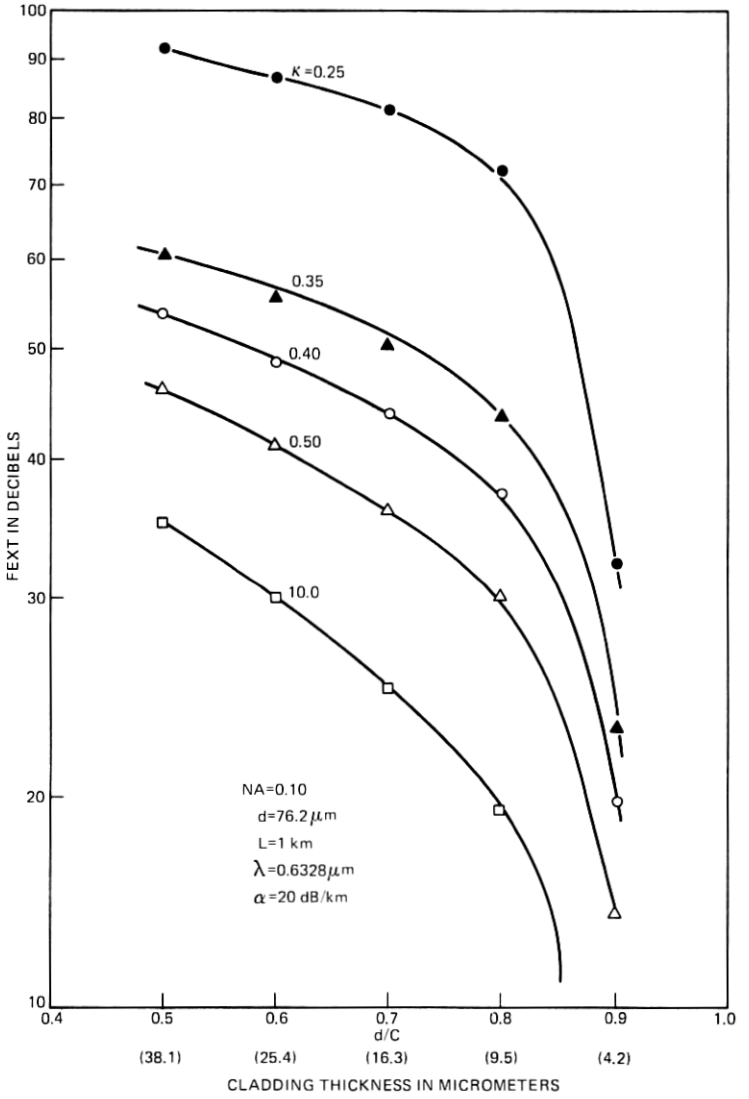

Fig. 15—FEXT vs. d/C (cladding thickness), $d = 76.2$ μm, NA = 0.10, $L = 1$ km, $\lambda = 0.6328$ μm, $\alpha = 20$ dB/km.

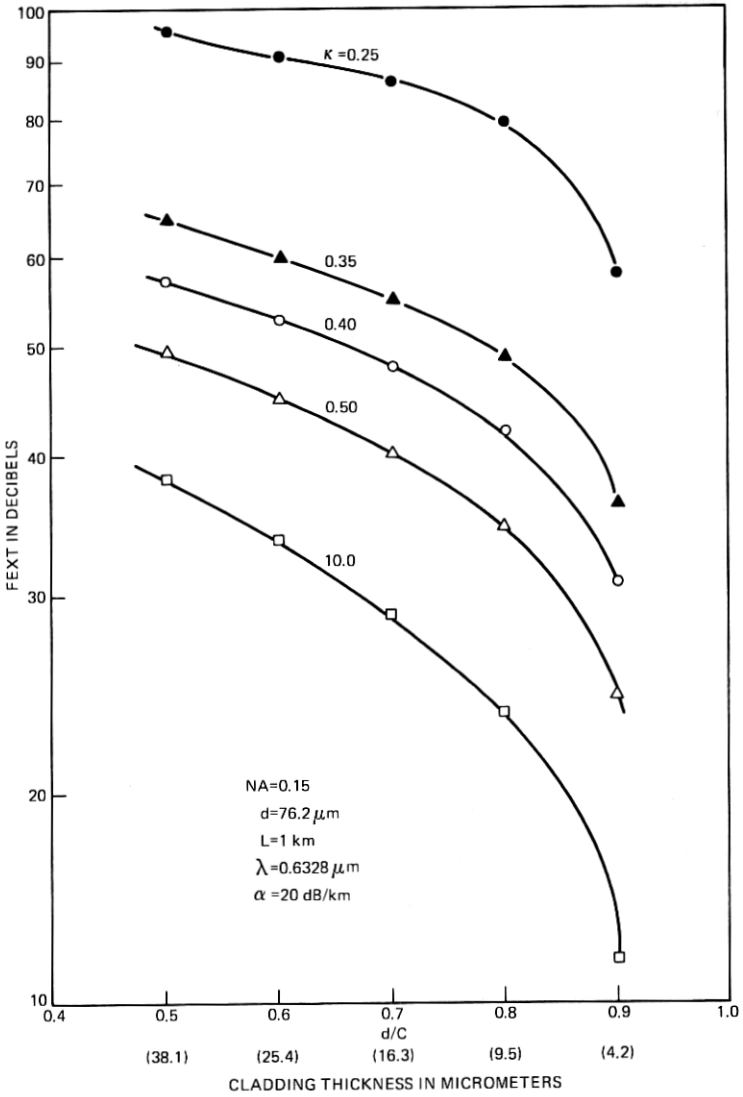

Fig. 16—FEXT vs. d/C (cladding thickness), $d = 76.2$ μm, NA = 0.15, $L = 1$ km, $\lambda = 0.6328$ μm, $\alpha = 20$ dB/km.

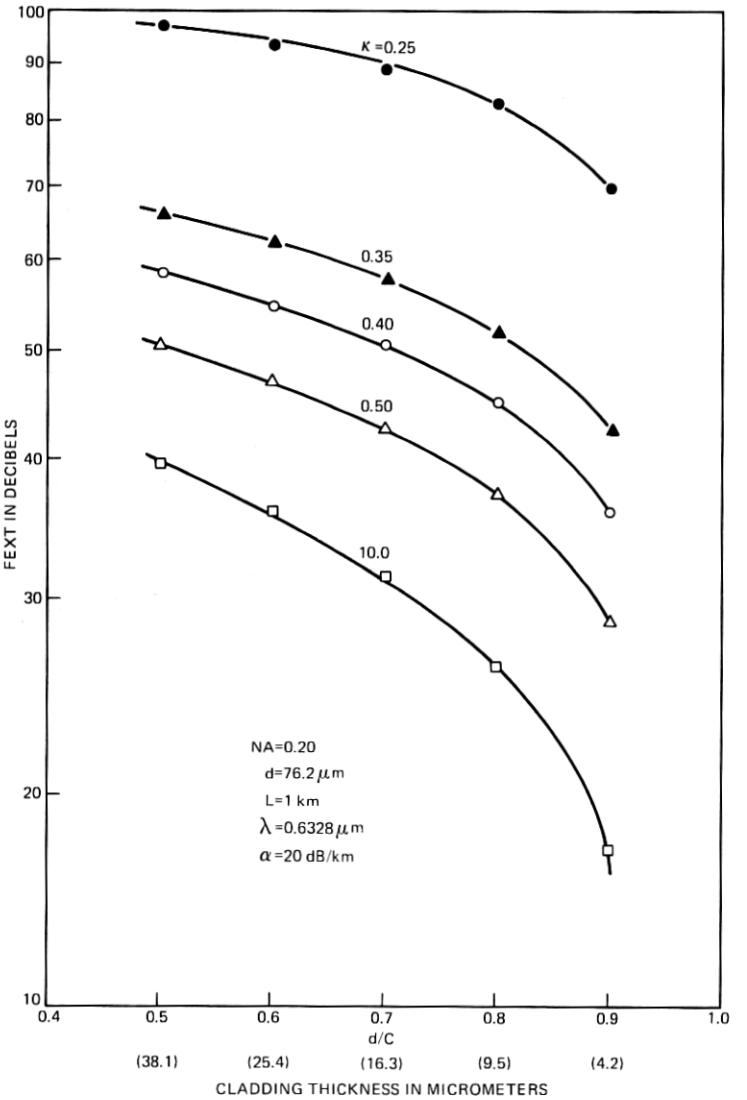

Fig. 17—FEXT vs. d/C (cladding thickness), $d = 76.2$ μm, NA = 0.20, $L = 1$ km, $\lambda = 0.6328$ μm, $\alpha = 20$ dB/km.

For practical claddings greater than 12 microns in thickness, increasing the cladding thickness will improve crosstalk isolation by approximately 0.8 dB/micron. Cladding thickness is an important design parameter for improving crosstalk isolation between optical fibers. If we attempted to eliminate crosstalk by coating the cladding with an opaque substance, cladding thickness would also play an

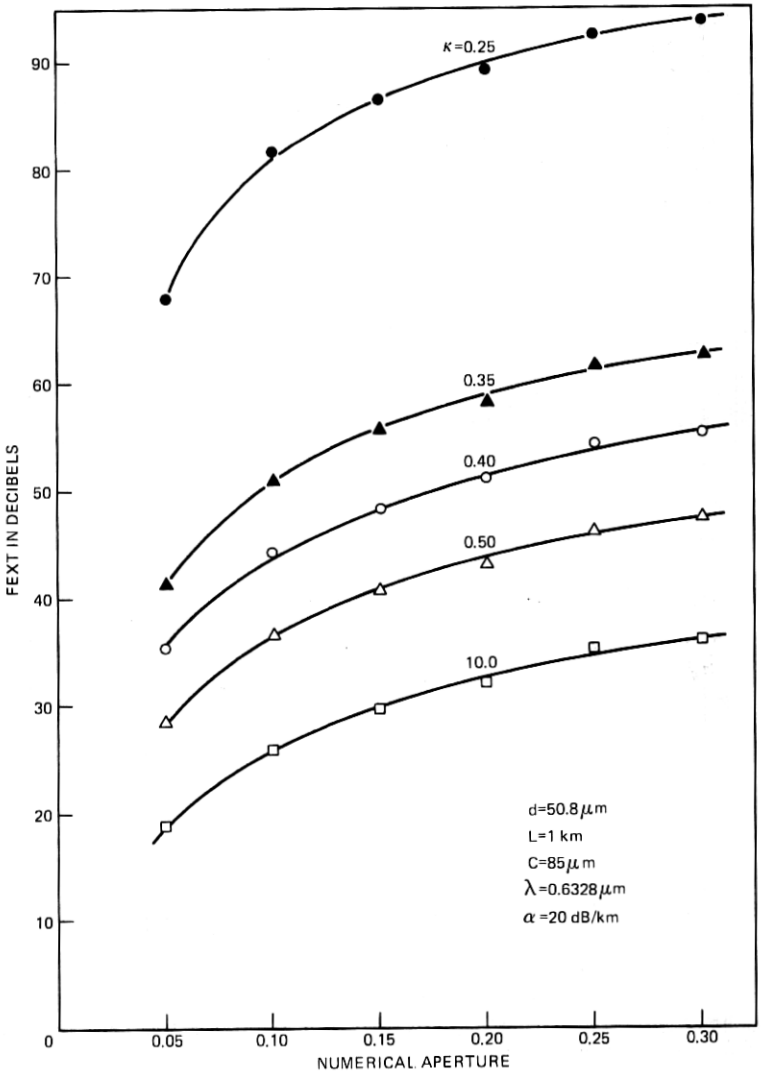

Fig. 18—FEXT vs. numerical aperture, $d = 50.8$ μm, $C = 85$ μm, $\alpha = 20$ dB/km, $L = 1$ km, $\lambda = 0.6328$ μm, $\kappa = 0.25, 0.35, 0.4, 0.5, 10.0$.

important role in determining the amount of loss suffered by the transmitted energy in the core owing to the lossy coating. A cross-check of Figs. 9 to 17 shows a very weak dependence of FEXT on core diameter.

A fiber core diameter of 50.8 μm and cladding diameter of 85 μm was chosen to represent a typical fiber geometry in the remainder of this study. Figure 18 shows the relationship between FEXT and numerical aperture with a fixed cladding refractive index of 1.458. For a given kappa, crosstalk isolation improves by approximately 6 dB by doubling the numerical aperture in the range from 0.10 to 0.30. For an NA

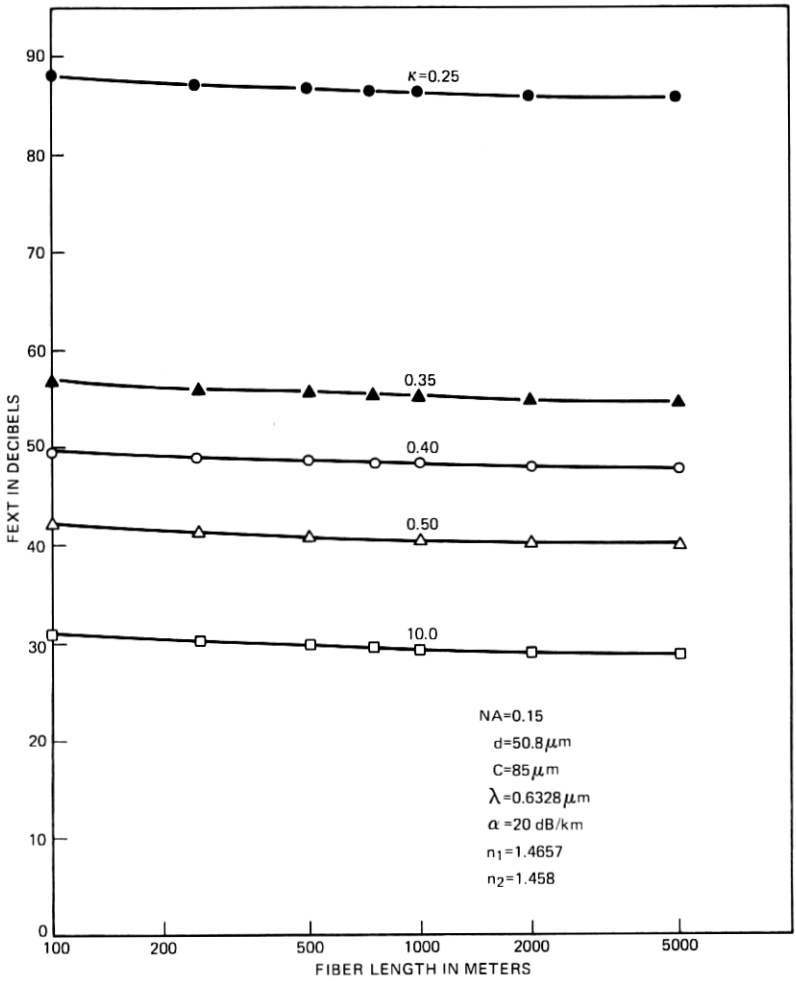

Fig. 19—FEXT vs. fiber length $d=50.8$ μm, $C=85$ μm, $\alpha=20$ dB/km, NA$=0.15$, $\lambda = 0.6328$ μm, $\kappa = 0.25, 0.35, 0.40, 0.50, 10.0$.

= 0.15, crosstalk was evaluated as a function of length as shown in Fig. 19. For a fixed kappa, crosstalk isolation decreased by approximately 2 dB per decade of length. The effect of kappa on crosstalk is shown in Fig. 20. Kappa is an indication of the distribution of power among the modes of the fiber. As kappa decreases in value, the energy distributed in the lower-order modes of a fiber increases. A knowledge of the steady-state mode distribution should enable us to estimate an effective κ for use in this model. As illustrated in Fig. 20, κ is an extremely important parameter in determining the crosstalk between fibers. For kappas less than 0.5, crosstalk isolation is greater than 40 dB for a kilometer length of fiber. For kappas less than 0.40, crosstalk isolation is greater than 50 dB. The final study, illustrated in Fig. 21, shows the relationship between FEXT and wavelength. For a given kappa, doubling the wavelength of the transmitting signal decreases crosstalk isolation by approximately 7 dB. It is envisioned that typical fiber losses in a future optical transmission system will be less than the 20-dB/km loss reported here. We will extend, in the future, our computer study to include fiber losses ranging from 2 to 20 dB/km, but do not expect this loss parameter to change the general conclusions drawn in this paper.

To determine if the primary mechanism for crosstalk in optical fibers is frustrated total reflection of waves in a multilayered medium, a crosstalk experiment on a long length of parallel fibers must be performed. In this experiment, crosstalk and kappa should be measured

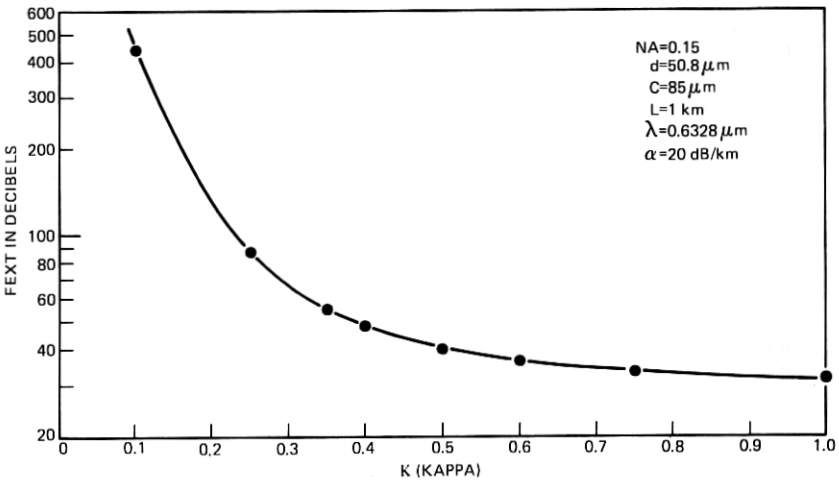

FIG. 20—FEXT vs. κ (kappa), L = 1 km, d = 50.8 μm, C = 85 μm, α = 20 dB/km, NA = 0.15, λ = 0.6328 μm.

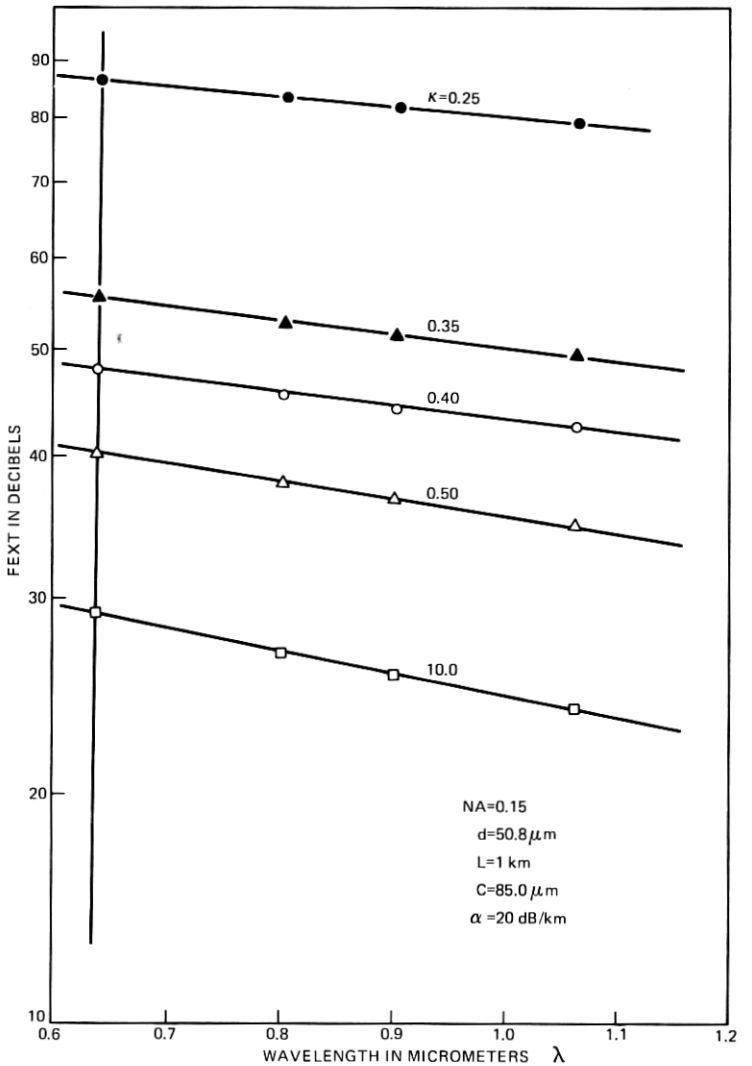

Fig. 21—FEXT vs. λ (wavelength), L = 1 km, d = 50.8 μm, C = 85 μm, α = 20 dB/km, NA = 0.15, κ = 0.25, 0.35, 0.40, 0.50, 10.0.

as a function of length at a number of different wavelengths. This type of experiment will enable us to check many aspects of the model.

APPENDIX A

Calculation of Transmission Coefficients in a Multilayered Medium

The general expression for the transmission coefficients in a multilayered dielectric medium is well known in the literature[15,17,18] and is

presented here. This expression is simplified for the three-medium case and, ultimately, eq. (16) in the text is derived.

Consider the geometry shown in Fig. 22. Let us suppose that between two semi-infinite media, denoted by 1 and $n + 1$, there are $n - 1$ layers of dielectric material denoted by 2, 3, $\cdots$, n. Let a plane wave be incident on the last layer at an angle of incidence θ_{n+1} and let the plane of incidence be the $x - z$ plane. As a result of multiple reflections at the boundaries of the layers, two waves exist in each medium with the exception of medium 1. Our problem will be to determine the amplitude of the transmitted wave in medium $n + 1$ and hence the transmission coefficient. The following notation will be used.

z_j = the coordinate of the boundary between the jth and $(j + 1)$st layers.
$d_j = z_j - z_{j-1}$ = the thickness of the jth layer.
$k_j = (2\pi/\lambda)(n_j)$ = the wave number in the jth medium.
$\alpha_j = k_j \cos \theta_j$ = z component of the wave vector in the jth layer.
$\phi_j = \alpha_j d_j$ = the phase change in the jth medium.
Z_j = the self-impedance of the jth layer.
Z_{in}^j = the input impedance looking into the jth medium from the $j + 1$ medium.

The electric and magnetic fields in the jth medium can then be written as

$$E_{jy} = A_j \exp\left[-i\alpha_j(Z - Z_{j-1})\right] + B_j \exp\left[i\alpha_j(Z - Z_{j-1})\right] \tag{29}$$

$$H_{jx} = \frac{1}{Z_j}\left\{A_j \exp\left[-i\alpha_j(Z - Z_{j-1})\right] - B_j \exp\left[i\alpha_j(Z - Z_{j-1})\right]\right\}. \tag{30}$$

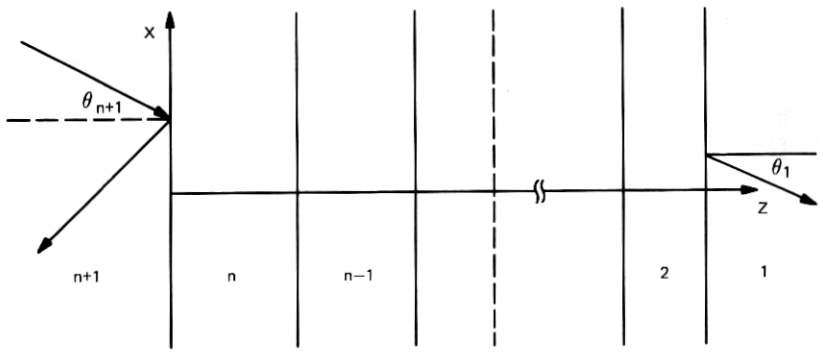

Fig. 22—Geometry used for calculation of transmission coefficients in multilayered dielectric media.

The x and t dependency in this case is omitted for the sake of brevity, but assumes the general form:

$$\exp i(k_{n+1}x \sin \theta_{n+1} - wt).$$

A_j and B_j, $B_1 = 0$ are the amplitudes of the incident and reflected waves in the jth medium. The amplitude A_{n+1} of the incident wave is assumed to be known. To obtain the transmission coefficient of interest,

$$\tau_{n+1} = \frac{A_1}{A_{n+1}} = \frac{A_1}{A_2}\frac{A_2}{A_3} \cdots \frac{A_{n-1}}{A_n}\cdot\frac{A_n}{A_{n+1}}. \tag{31}$$

We can write $2n$ boundary equations for the tangential components of the fields and solve these equations for $A_1, A_2, \cdots, A_{n+1}$; $B_1, B_2, \cdots, B_{n+1}$. When these coefficients are known, the transmission and reflection coefficients for the multilayered medium are obtained.

A second approach, and one that develops an iterative scheme more suitable to a digital computer, describes the transmission coefficient in terms of a generalized input impedance.[19] This is the approach that will be followed here. It is straightforward to derive, and it is shown in the literature that:

$$\frac{A_j}{A_{j+1}} = \frac{Z_j + Z_{\text{in}}^j}{Z_{j+1} + Z_{\text{in}}^j} \exp (i\phi_j). \tag{32}$$

Substituting into eq. (31) yields

$$\tau_{n+1} = \prod_{j=1}^{j=n} \frac{Z_j + Z_{\text{in}}^j}{Z_{j+1} + Z_{\text{in}}^j} \exp (i\phi_j), \tag{33}$$

with $d_1 = 0$, where

$$Z_{\text{in}}^j = \frac{Z_{\text{in}}^{j-1} - iZ_j \tan \phi_j}{Z_j - iZ_{\text{in}}^{j-1} \tan \phi_j}\cdot Z_j. \tag{34}$$

Specializing eq. (33) for the three-medium case discussed in the text, we can obtain, with some algebraic manipulation, the following formula:

$$\tau_2 = \frac{4Z_1Z_2}{(Z_1 - Z_2)(Z_2 - Z_3)\epsilon^{i\phi_2} + (Z_1 + Z_2)(Z_2 + Z_3)\epsilon^{-i\phi_2}}. \tag{35}$$

For electric fields parallel and perpendicular to the plane of incidence, eq. (35) will take different forms. For $E_\perp$,

$$Z_1 = \frac{Z_o}{n_1 \cos \theta_1} = Z_3 \tag{36}$$

$$Z_2 = \frac{Z_o}{n_2 \cos \theta_2} = \frac{Z_o}{in_2\gamma}, \tag{37}$$

where

$$\gamma = \left[\left(\frac{n_3}{n_2}\right)^2 \sin^2\theta_1 - 1\right]^{\frac{1}{2}} \tag{38}$$

$$Z_o = \sqrt{\frac{\mu}{\epsilon}} \tag{39}$$

$$\beta = k_2 d_2 \gamma. \tag{40}$$

After some algebraic manipulation,

$$\tau_{2\perp} = \frac{K_1^2 \cosh\beta - iK_1K_2 \sinh\beta}{K_1^2 \cosh^2\beta + K_2^2 \sinh^2\beta}, \tag{41}$$

where

$$K_1 = 2n_1n_2 \cos\theta_1\gamma \tag{42}$$

$$K_2 = n_2^2\gamma^2 - n_1^2 \cos^2\theta_1, \tag{43}$$

for E_{11}

$$Z_1 = \frac{Z_o \cos\theta_1}{n_1} = Z_3 \tag{44}$$

$$Z_2 = \frac{Z_o \cos\theta_2}{n_2} = \frac{iZ_o\gamma}{n_2}, \tag{45}$$

and $T_{2_{11}}$ becomes

$$\tau_{2_{11}} = \frac{K_1^2 \cosh\beta + iK_1K_3 \sinh\beta}{K_1^2 \cosh^2\beta + K_3^2 \sinh^2\beta}, \tag{46}$$

where

$$K_3 = n_2^2 \cos^2\theta_1 - \gamma^2 n_1^2. \tag{47}$$

Utilizing eqs. (41) and (46), we can obtain the power transmission coefficients directly:

$$T_{2\perp} = |\tau_{2\perp}|^2 = \frac{1}{\cosh^2\beta + [(n_2^2\gamma^2 - n_1^2\cos^2\theta_1)/2n_1n_2\cos\theta_1\gamma]^2 \sinh^2\beta} \tag{48}$$

$$T_{2_{11}} = |\tau_{2_{11}}|^2 = \frac{1}{\cosh^2\beta + [(n_2^2\cos^2\theta_1 - \gamma^2 n_1^2)/2\cos\theta_1 n_1 n_2\gamma]^2 \sinh^2\beta}. \tag{49}$$

Equations (48) and (49) were used to obtain eq. (17) in the text of this paper.

REFERENCES

1. A. W. Snyder, "Coupled-Mode Theory for Optical Fibers," J. Opt. Soc. Am., *62*, No. 11 (November 1972), pp. 1267–1277.
2. D. Marcuse, "The Coupling of Degenerate Modes in Two Parallel Dielectric Waveguides," B.S.T.J., *50*, No. 6 (July–August 1971), pp. 1791–1816.

3. A. L. Jones, "Coupling of Optical Fibers and Scattering in Fibers," J. Opt. Soc. Am., *55*, No. 3 (March 1965), pp. 261–271.
4. D. Marcuse, *Light Transmission Optics*, New York: Van Nostrand Reinhold Co., 1972.
5. R. Vanclooster and P. Phariseau, "The Coupling of Two Parallel Dielectric Fibers I—Basic Equations," Physica, *47*, No. 4 (June 1970), pp. 485–500.
6. R. Vanclooster and P. Phariseau, "The Coupling of Two Dielectric Fibers II—Characteristic of Coupling in Two Fibers," Physica, *47*, No. 4 (June 1970), pp. 501–514.
7. R. Vanclooster and P. Phariseau, "Light Propagation in Fiber Bundles," Physica, *49*, No. 4 (November 1970), pp. 493–501.
8. M. Matsuhara and N. Kumagai, "Theory of Coupled Open Transmission Lines and Its Applications," IEEE Trans. Microwave Theory Tech., *MTT-22*, No. 4, April, 1974.
9. D. Marcuse, "Crosstalk Caused by Scattering in Slab Waveguides," B.S.T.J., *50*, No. 6 (July–August 1971), pp. 1817–1831.
10. H. P. Yuen, unpublished work.
11. N. S. Kapany and J. J. Burke, *Optical Waveguides*, New York: Academic Press, 1972.
12. N. S. Kapany, *Fiber Optics, Principles and Applications*, New York: Academic Press, 1967.
13. N. S. Kapany and J. J. Burke, "Fiber Optics IX, Waveguide Effects," J. Opt. Soc. Am., *51*, No. 10 (October 1961), pp. 1067–1078.
14. N. S. Kapany, "Fiber Optics V, Light Leakage due to Frustrated Total Reflection," J. Opt. Soc. Am., *49*, No. 9 (August 1959), pp. 770–778.
15. L. M. Brekhovskikh, *Waves in Layered Media*, New York: Academic Press, 1960.
16. R. H. Renard, "Total Reflection, A New Evaluation of the Goos-Hänchen Shift," J. Opt. Soc. Am., *54*, No. 10 (October 1964), pp. 1190–1197.
17. W. Culshaw, "Stratified Media and Total Reflection Phenomena," Appl. Opt., *11*, No. 11 (November 1972), pp. 2639–2648.
18. M. Born and E. Wolf, *Principles of Optics*, New York: Pergammon Press, 1970.
19. B. Carnahan, H. A. Luther, and J. O. Wilkes, *Applied Numerical Methods*, New York: John Wiley, 1969.